Chemical Engineering Journal 240 (2014) 290–306

Contents lists available at ScienceDirect

Chemical Engineering Journal

journal homepage: www.elsevier.com/locate/cej

X-ray micro-tomography and pore network modeling of single-phase fixed-bed reactors

F. Larachi [a,*], R. Hannaoui [a], P. Horgue [b], F. Augier [a], Y. Haroun [a], S. Youssef [c], E. Rosenberg [c], M. Prat [b,d], M. Quintard [b,d]

[a] IFP Energies nouvelles-Lyon, Rond-point de l'échangeur de Solaize, BP 3, 69360 Solaize, France
[b] Université de Toulouse, INPT, UPS, Institut de Mécanique des Fluides de Toulouse, allée Camille Soula, 31400 Toulouse, France
[c] IFP Energies nouvelles, 1 et 4 avenue Bois-Préau, 92852 Rueil-Malmaison, France
[d] CNRS, IMFT, F-31400 Toulouse, France

HIGHLIGHTS

- 3D pore network extracted from X-ray μ-tomography imaging of a bead pack.
- Non-Darcy flow simulated using pore-throat-pore mesoscopic elements.
- Dissipation dissected into elementary pore/channel linear and quadratic effects.
- Back-mixing *via* channel retroflow identified and quantified by network model.

GRAPHICAL ABSTRACT

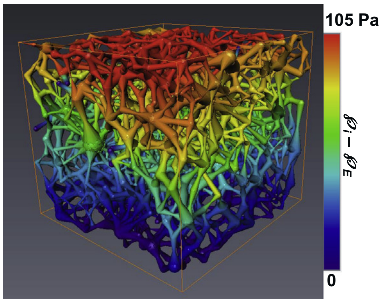

ARTICLE INFO

Article history:
Received 26 September 2013
Received in revised form 23 November 2013
Accepted 26 November 2013
Available online 4 December 2013

Keywords:
Pore networks
Porous media
Single-phase flow
Non-Darcy flow
Inertial effects
Mechanical dispersion

ABSTRACT

A three-dimensional (3D) irregular and unstructured pore network was built using local topological and geometrical properties of an isometric bead pack imaged by means of a high-resolution X-ray computed micro-tomography technique. A pore network model was developed to analyze the 3D laminar/inertial (non-Darcy) flows at the mesoscopic (pore level) and macroscopic (after ensemble-averaging) levels. The non-linear laminar flow signatures were captured at the mesoscale on the basis of analogies with contraction and expansion friction losses. The model provided remarkably good predictions of macroscopic frictional loss gradient in Darcy and non-Darcy regimes with clear-cut demarcation using channel-based Reynolds number statistics. It was also able to differentiate contributions due to pore and channel linear losses, and contraction/expansion quadratic losses. Macroscopic mechanical dispersion was analyzed in terms of retroflow channels, and transverse and longitudinal Péclet numbers. The model qualitatively retrieved the Péclet-Reynolds scaling law expected for heterogeneous networks with predominance of mechanical dispersion. Advocated in watermark is the potential of pore network modeling to build *a posteriori* constitutive relations for the closures of the more conventional macroscopic Euler approaches to capture more realistically single-phase flow phenomena in fixed-bed reactor applications in chemical engineering.

---

* Corresponding author. Address: Department of Chemical Engineering, Laval University, Québec, QC G1V 0A6, Canada. Tel.: +1 418 656 3566; fax: +1 418 656 5993.
E-mail address: faical.larachi@gch.ulaval.ca (F. Larachi).

1385-8947/$ - see front matter © 2013 Elsevier B.V. All rights reserved.
http://dx.doi.org/10.1016/j.cej.2013.11.077

Nomenclature

A_{ij}	channel friction loss per unit length, Pa/m
C_0	laminar constant (Eq. (11)), –
C_{ij}	contraction friction loss, Pa
D_0	laminar constant (Eq. (12)), –
d	particle diameter, m
E_{ij}	expansion friction loss, Pa
Eu_{ij}	channel ij Euler number, –
e	bed porosity, –
g	gravitational acceleration, m/s^2
L_{ij}	center-of-mass distance between two adjacent pores, m
l_{ij}	equivalent channel length, m
m	curvature parameter (Eq. (12)) or number of channels entering a given pore, –
N_c	total number of channels, –
N_p	total number of pores, –
n	curvature parameter (Eq. (11)), –
P_F	network feed pressure, Pa
P_E	network exit pressure, Pa
p'_i	channel static pressure from pore i side, Pa
P_i	pore i static pressure, Pa
$\wp_i$	pore i total head, Pa
Pe_L	longitudinal channel Péclet number, $\langle v_{c\alpha}\rangle/\langle v_{c\alpha}\rangle$, – (same formalism for pore)
Q	cumulative (feed) flow rate, m^3/s
p	number of channels leaving a given pore, –
q_{ij}	channel ij volumetric flux, m^3/s
Re_{bed}	bed (or particle) Reynolds number, $\rho V_s d/(1-e)\mu$, (as in traditional definition of packed-bed friction factor-Re correlations), –
Re_{ij}	channel ij Reynolds number (Eq. (13)), –
r_i	pore i radius, m
r_{cij}	channel ij constriction radius, m
r^e_{cij}	channel ij effective constriction radius, m
r_{minij}	channel ij minimum throat radius, m
U_α	directional unit vector of pore flow (Eq. (27)), –
V_s	superficial velocity, m/s
v_{ij}	channel ij interstitial velocity (Eq. (28)), m/s
$\langle v_{c\alpha}\rangle$	ensemble-average channel ($\alpha = x, y, z$) velocity component, m/s
$\langle v'_{c\alpha}\rangle$	ensemble-average channel ($\alpha = x, y, z$) root-mean-square velocity component, m/s
$\langle v_{p\alpha}\rangle$	ensemble-average pore ($\alpha = x, y, z$) velocity component, m/s
$\langle v'_{p\alpha}\rangle$	ensemble-average pore ($\alpha = x, y, z$) root-mean-square velocity component, m/s
(x_i,y_i,z_i)	pore i center-of-mass coordinates, m

Greek

Γ_{y-}	lower network domain exit boundary
Γ_{y+}	upper network domain entrance boundary
$\gamma_0 \cup \gamma_{s0} \cup \gamma_1$	constriction contour
$\gamma_1 \cup \gamma_{s1} \cup \gamma_2$	channel contour
$\gamma_2 \cup \gamma_{s2} \cup \gamma_3$	expansion contour
Δx	spatial resolution, µm
δ_j	pore j multiplier, –
ε_{ij}	channel ij expansion friction loss factor, –
κ_{ij}	channel ij contraction friction loss factor, –
μ	fluid viscosity, Pa s
ρ	fluid density, kg/m^3
σ	standard-deviation, Table 1
$\underline{\phi}$	volumetric flux objective function vector, m^3/s

Subscript

c	channel
E	exit
F	feed
L	longitudinal
p	pore
T	transverse

Superscript

$'$	relative to channel
—	volume average operator (Eq. (23))
(i)→	leaving pore i (Eq. (26))
_	vector entity
=	matrix entity

Acronym

⟨⟩	ensemble-average operator
3D(2D)	three (two) dimensional
COV	coefficient of variation, Table 1
CSTR	continuous-stirred tank reactor

1. Introduction

Pore network modeling is a remarkably powerful approach which allows linking pore-level transport phenomena to the macroscale flow behavior in porous media [1]. Since its inception with the seminal works by Fatt [2], the literature on pore network modeling has been growing at a phenomenal rate and, hitherto, has imposed itself as a key branch of research on porous media. The breadth of possibilities allowed by pore network modeling extends from procurement of upscaled intrinsic and relative permeabilities [3–5], estimation of hydrodynamic dispersion and mass transfer with or without phase changes [1,6–9], and simulation of quasi-equilibrium and non-equilibrium drainage and imbibition dynamics [10,11], to name just a few topics.

It is the advent of spatially-resolved imaging techniques, such as X-ray computed micro-tomography, that has thrust the capabilities of network modeling to new heights [1]. Nowadays, these techniques enable imaging the 3D pore space of actual porous media with routine spatial resolutions down to a micron [12]. Topologically equivalent backbones are then extracted whereby the irregular poral space is represented in the form of bonds and nodes to which volumes, areas, lengths, and shapes are assigned to mimic the detailed 3D images. Hence, the level of scrutiny, in its default assertion, is meant to depict mesoscale (or pore-level) physics in accordance with which network modeling relies on a collection of simple physical rules, *e.g.*, mass, momentum and energy balances, tinged with the *local* topological and geometrical attributes belonging to each individual pore. Often, pore network modeling refers to instances where the microscale inner-pore-level information is either forgone or compressed in the averaging processes – *e.g.*, in the form of shape factors, flow rates in idealized channel geometry, *etc.* In this regard, pore network modeling bridges the gap between the macroscopic volume-average multi-fluid Euler approaches that necessitate *a priori* knowledge of constitutive relationships [13–16], and the higher-rank CPU-intensive simulation methods, such as lattice Boltzmann [17], smoothed